

Medulloblastoma: correlation among findings of conventional magnetic resonance imaging, diffusion-weighted imaging and proton magnetic resonance spectroscopy*

Medulloblastoma: correlação entre ressonância magnética convencional, difusão e espectroscopia de prótons

Mariana Vieira de Melo da Fonte¹, Raquel Portugal Guimarães Amaral¹, Maria Olívia Rodrigues Costa², Maria Concepción Garcia Otaduy³, Leandro Tavares Lucato⁴, Umbertina Conti Reed⁵, Sergio Rosemberg⁶, Claudia da Costa Leite⁷

Abstract **OBJECTIVE:** To correlate imaging findings of medulloblastomas at conventional magnetic resonance imaging, diffusion-weighted imaging and proton magnetic resonance spectroscopy, comparing them with data in the literature. **MATERIALS AND METHODS:** Preoperative magnetic resonance imaging studies of nine pediatric patients with histologically confirmed medulloblastomas (eight desmoplastic medulloblastoma, and one giant cell medulloblastoma) were retrospectively reviewed, considering demographics as well as tumors characteristics such as localization, morphology, signal intensity, contrast-enhancement, dissemination, and diffusion-weighted imaging and spectroscopy findings. **RESULTS:** In most of cases the tumors were centered in the cerebellar vermis (77.8%), predominantly solid (88.9%), hypointense on T1-weighted images and intermediate/hyperintense on T2-FLAIR-weighted images, with heterogeneous enhancement (100%), tumor dissemination/extension (77.8%) and limited water molecule mobility (100%). Proton spectroscopy acquired with STEAM technique ($n = 6$) demonstrated decreased Naa/Cr ratio (83.3%) and increased Co/Cr (100%) and ml/Cr (66.7%) ratios; and with PRESS technique ($n = 7$) demonstrated lactate peak (57.1%). **CONCLUSION:** Macroscopic magnetic resonance imaging findings in association with biochemical features of medulloblastomas have been useful in the differentiation among the most frequent posterior fossa tumors. **Keywords:** Medulloblastoma; Infratentorial neoplasms; Pediatric brain tumors; Magnetic resonance imaging; Diffusion-weighted magnetic resonance imaging; Magnetic resonance spectroscopy.

Resumo **OBJETIVO:** Correlacionar os achados de ressonância magnética convencional, difusão e espectroscopia de prótons nos medulloblastomas, e compará-los aos dados da literatura. **MATERIAIS E MÉTODOS:** Análise retrospectiva de exames de ressonância magnética pré-operatórios de nove pacientes na faixa pediátrica com diagnóstico histológico de medulloblastoma (oito desmoplásicos e um de células gigantes). Foram considerados dados demográficos e características do tumor como localização, característica morfológica, intensidade de sinal, realce, disseminação e achados na difusão e espectroscopia. **RESULTADOS:** Na maioria dos casos os tumores apresentaram epicentro no vermis cerebelar (77,8%), sendo predominantemente sólido (88,9%), com hipossinal nas seqüências ponderadas em T1 e iso/hipersinal nas seqüências ponderadas em T2 e FLAIR, realce heterogêneo (100%), sinais de disseminação/extensão tumoral (77,8%) e restrição à movimentação das moléculas de água (100%). A espectroscopia de prótons pela técnica STEAM ($n = 6$) demonstrou redução da relação Naa/Cr (83,3%) e aumento de Co/Cr (100%) e ml/Cr (66,7%), e pela técnica PRESS ($n = 7$) evidenciou pico de lactato (57,1%). **CONCLUSÃO:** O conjunto dos achados macroscópicos obtidos pela ressonância magnética, somado às características bioquímicas dos medulloblastomas, têm sido úteis na tentativa de diferenciação entre os principais tumores da fossa posterior. **Unitermos:** Medulloblastoma; Neoplasias infratentoriais; Tumores cerebrais pediátricos; Imagem por ressonância magnética; Imagem de difusão por ressonância magnética; Espectroscopia de prótons.

Fonte MVM, Amaral RPG, Costa MOR, Otaduy MCG, Lucato LT, Reed UC, Rosemberg S, Leite CC. Medulloblastoma: correlation among findings of conventional magnetic resonance imaging, diffusion-weighted imaging and proton magnetic resonance spectroscopy. Radiol Bras. 2008;41(6):373-378.

* Study developed in the Unit of Magnetic Resonance Imaging – Instituto de Radiologia do Hospital das Clínicas da Faculdade de Medicina da Universidade de São Paulo (InRad/HC-FMUSP), São Paulo, SP, Brazil.

1. MDs, Radiologists, Researchers at Unit of Magnetic Resonance Imaging – Instituto de Radiologia do Hospital das Clínicas da Faculdade de Medicina da Universidade de São Paulo (InRad/HC-FMUSP), São Paulo, SP, Brazil.

2. PhD, Department of Radiology, Faculdade de Medicina da Universidade de São Paulo (FMUSP), São Paulo, SP, Brazil.

3. PhD, Physicist at Unit of Magnetic Resonance Imaging – Instituto

de Radiologia do Hospital das Clínicas da Faculdade de Medicina da Universidade de São Paulo (InRad/HC-FMUSP), São Paulo, SP, Brazil.

4. PhD, Physician Assistant at Unit of Magnetic Resonance Imaging – Instituto de Radiologia do Hospital das Clínicas da Faculdade de Medicina da Universidade de São Paulo (InRad/HC-FMUSP), São Paulo, SP, Brazil.

5. Full Professor, Unit of Pediatric Neurology, Department of Neurology – Faculdade de Medicina da Universidade de São Paulo (FMUSP), São Paulo, SP, Brazil.

6. Private Docent, Associate Professor, Physician Assistant at De-

partment of Pathology – Hospital das Clínicas da Faculdade de Medicina da Universidade de São Paulo (HC-FMUSP), São Paulo, SP, Brazil.

7. Private Docent, Associate Professor, Head for the Unit of Magnetic Resonance Imaging – Instituto de Radiologia do Hospital das Clínicas da Faculdade de Medicina da Universidade de São Paulo (InRad/HC-FMUSP), São Paulo, SP, Brazil.

Mailing address: Dra. Mariana Vieira de Melo da Fonte. Avenida João Castaldi, 155, ap.174, Indianópolis. São Paulo, SP, Brazil, 04517-050. E-mail: mvmfonte@uol.com.br.

Received October 7, 2007. Accepted after revision August 12, 2008.

INTRODUCTION

Tumors of the central nervous system correspond to approximately 20% of all neoplasms in the pediatric age group, and this is the second most common type of pediatric cancer surpassed in incidence only by leukemia⁽¹⁾.

Medulloblastoma is a primitive neuroectodermal tumor typically occurring in the posterior fossa in children⁽²⁾. This tumor accounts for 30%–40% of posterior fossa tumors in children, where it is most commonly found, and for 15%–25% of all pediatric brain tumors. In adults, this tumor accounts for 1% of the brain tumors⁽³⁾.

This tumor is a highly malignant and fast-growing neoplasm⁽⁴⁾. Histological variations include: classic medulloblastoma, desmoplastic medulloblastoma, cerebellar neuroblastoma, large-cell medulloblastoma, medulloblastoma and melanotic medulloblastoma⁽¹⁾.

Imaging methods play an essential role in the diagnosis and therapeutic planning for patients with intracranial tumors. Magnetic resonance imaging (MRI), in particular, has emerged as the imaging method most frequently utilized for evaluating intracranial tumors, playing an increasing and significant role in these cases. Advanced resources can be integrated into the conventional techniques, adding physiological and biochemical data to anatomical information to improve the accuracy of the method. Among these techniques, diffusion sequences and proton spectroscopy can be mentioned⁽⁵⁾.

Radiologically, medulloblastomas present a morphology similar to many other tumors, such as cerebellar astrocytomas, ependymomas or yet meningiomas which should be considered in the differential diagnosis of any posterior fossa mass in children or young adults⁽⁶⁾.

Considering the frequency of medulloblastomas in children and the difficulty in the definition of a differential diagnosis among posterior fossa tumors in this age range, the authors have proposed a retrospective analysis of preoperative studies of nine pediatric patients with medulloblastoma, and correlation of findings of conventional MRI, diffusion sequences and proton spectroscopy in comparison with data reported in the literature.

MATERIALS AND METHODS

Preoperative MRI studies of nine pediatric patients with histopathologically confirmed diagnosis of medulloblastoma (eight desmoplastic and one anaplastic large-cell type) were retrospectively evaluated. These studies were performed in the Unit of Magnetic Resonance Imaging at Instituto de Radiologia do Hospital das Clínicas da Faculdade de Medicina da Universidade de São Paulo (InRad/HC-FMUSP), along a four-year period. The present study was developed in compliance with the World Medical Association Declaration of Helsinki Principles for Medical Research Involving Human Subjects.

All the studies were performed in a 1.5 T equipment (General Electric Medical Systems; Milwaukee, USA), with 5 mm-thick slices, utilizing the techniques spin-echo (SE) with T1-weighted sequence (366–500 ms/9–14 ms [repetition time/echo time – TR/TE]), axial plane in all of the cases and sagittal in seven cases; fast spin-echo (FSE) with T2-weighted sequence (4,500–5,100 ms/99–102 ms – TR/TE), axial plane in seven cases, coronal in three and axial with fat-saturation in two cases; fluid-attenuated inversion recovery (FLAIR) (8,402–10,002 ms/110–157 ms/2.200 ms – TR/TE/TI [inversion time]), axial plane in all of the cases. After intravenous paramagnetic contrast injection (gadolinium at the usual dose of 0.1 mmol/kg), the T1-weighted sequence was repeated in the axial, coronal and sagittal planes for all the nine patients. Advanced techniques such as diffusion sequence and proton spectroscopy were utilized in nine and seven patients respectively. Diffusion sequences were acquired previously to the paramagnetic contrast injection, utilizing b values = 0 and 1.000 s/mm² applied in the X, Y and Z directions. Spectroscopy was performed with the techniques stimulated echo acquisition mode (STEAM) (1,500 ms/30 ms) and point resolved spectroscopy (PRESS) (1,500 ms/135 ms), for seven patients, with a single voxel on the lesion. The STEAM technique was utilized for evaluation of the metabolites ratio [N-acetyl aspartate/creatine (Naa/Cr), choline/creatine (Co/Cr) and myo/inositol/creatine (mI/Cr)], while the PRESS technique determined the lactate (Lac) peak.

The images were analyzed on an Advantage-GE workstation (General Electric Medical Systems; Milwaukee, USA) for reconstruction of a map of apparent diffusion coefficient (ADC) and study of the spectroscopy graphic. Demographic data such as age and sex were considered as well as data inherent to the tumor: localization, morphology, signal intensity, enhancement, tumor dissemination, features on the diffusion sequence and spectroscopic findings (Naa/Cr, Co/Cr, mI/Cr ratios and presence of Lac peak).

Metabolites ratios (Naa/Cr, Co/Cr and mI/Cr) were compared with a control group, whose data had been previously collected. The casuistic included 37 (22 male and 15 female) healthy individuals with ages ranging between three and 18 years submitted to spectroscopic study with voxel on the cerebellar hemisphere. These individuals had no neurological complaints or symptoms, their skull MRI studies were normal and their inclusion in the present study was authorized by their legal representatives (Table 1)⁽⁷⁾.

RESULTS

The casuistic included six girls (66.7%) and three boys (33.3%) with ages ranging between two and 19 years (mean = 8.5 years), six of them (66.7%) with ages ≤ 10 years.

The tumor was localized in the posterior fossa in all of the nine patients, with the epicenter in the cerebellar vermis, extending anteriorly towards the IV ventricle in seven (77.8%) (including two adolescents with 12 and 19 years of age); with involvement of the right cerebellar vermis and

Table 1 Metabolites ratios (Naa/Cr, Co/Cr and mI/Cr) evaluated by the STEAM and PRESS techniques, performed in the control group with voxel on the cerebellar hemisphere.

	Technique	n	Metabolites
Naa/Cr	STEAM	25	1.07 ± 0.22
	PRESS	37	1.47 ± 0.27
Co/Cr	STEAM	37	0.87 ± 0.17
	PRESS	37	1.12 ± 0.19
mI/Cr	STEAM	37	0.64 ± 0.12

n, number of sample; Naa, N-acetyl aspartate; Cr, creatine; Co, choline; mI, myo-inositol; STEAM, stimulated echo acquisition mode; PRESS, point resolved spectroscopy.

hemisphere in a four-year-old child (11.1%); and on the IV ventricle/encephalic trunk topography in one case (11.1%).

In most of cases (88.9%) the tumors were predominantly solid. Hypointense signal was observed on T1-weighted sequences, and iso- or hyperintense signal on T2-weighted and FLAIR sequences as related to the brain gray matter. All the tumors were heterogeneous, possibly because of the presence of cysts/necrosis, with the maximum diameter of the cystic/necrotic area reaching 3.4 cm. Heterogeneous en-

hancement was observed in all of the cases, ranging from moderate to intense, and from partial to total (Figure 1). In the preoperative evaluation, dissemination through the cerebrospinal fluid was present in six patients (66.7%) (Figure 2). Extension to the Luschka's foramen was observed in four patients (44.4%), one of them with concomitant involvement of the Magendie's foramen (Table 2). Diffusion sequence demonstrated areas with restricted water molecules mobility in all of the nine cases ($n = 9$) (Figure 3). At the STEAM proton

spectroscopy ($n = 7$), the evaluation of metabolites ratio could not be performed in one case, possibly because of the magnetic field heterogeneity and consequential decrease in the signal/noise ratio; in this case, the metabolites ratio was classified as indeterminate. In the other six cases, spectroscopy demonstrated a decrease in the Naa/Cr ratio in 83.3%, increase in the Co/Cr ratio in 100%, and increase in the mI/Cr ratio in 66.7% (Figure 4). The PRESS technique showed the lactate peak in 57.1% of the seven cases evaluated (Table 3).

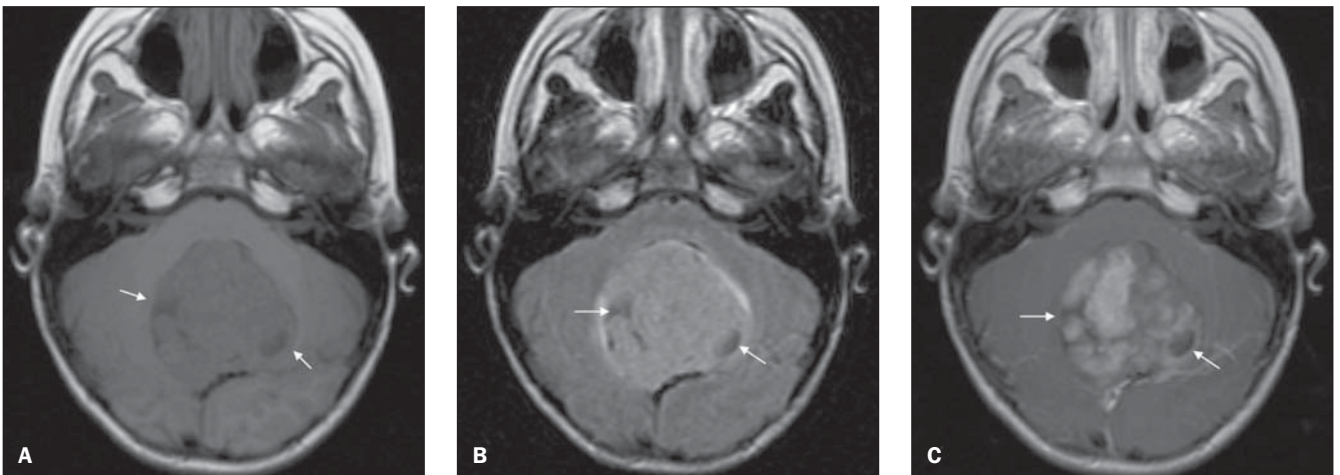


Figure 1. Medulloblastoma in a four-year old girl. Axial magnetic resonance images demonstrate a predominantly solid mass on the posterior fossa midline, with the epiventer in the cerebellar vermis, extending anteriorly to the IV ventricle. The mass is heterogeneous, with a subtle hypointense signal on T1-weighted sequence (A), hyperintense signal on FLAIR sequence (B) and partial/heterogeneous gadolinium-based contrast enhancement (C). Note the presence of intermingled cysts/necrosis (arrows).

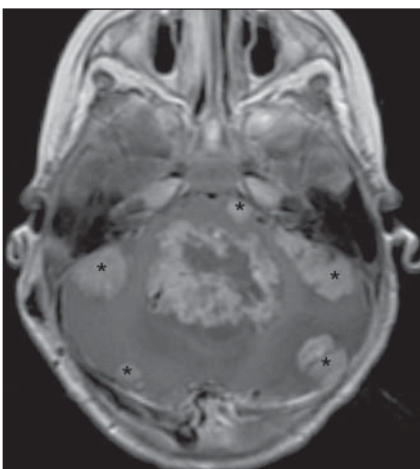


Figure 2. Medulloblastoma in a two-year-old girl. Axial magnetic resonance, T1-weighted image acquired after gadolinium injection, demonstrating an expansile mass on the posterior fossa midline, with intense and heterogeneous enhancement. Signs of tumor dissemination characterized by nodular meningeal enhancement (asterisks).

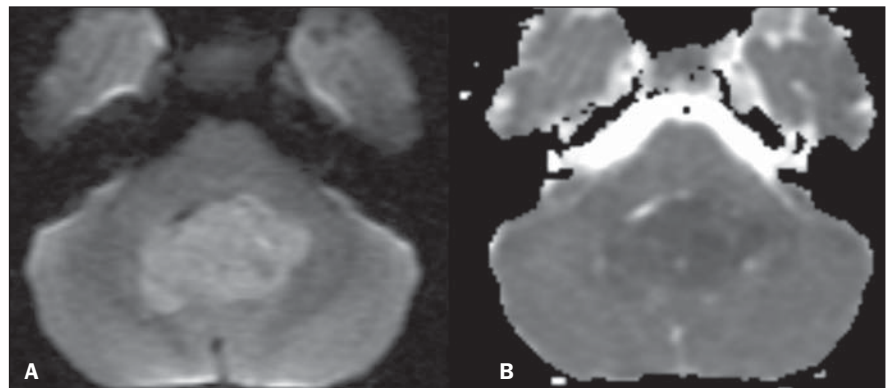


Figure 3. Medulloblastoma in a four-year-old girl. Diffusion sequence (at left) demonstrates hyperintense signal from an expansile lesion on the posterior fossa midline. The ADC map reconstruction (at right) demonstrates predominant hypointense signal characterizing restriction to water molecules mobility.

Table 2 – Evaluation of medulloblastomas by MRI considering morphology, signal intensity, presence of enhancement and dissemination pattern.

	n	%
Morphological characteristic		
Predominantly solid	8	88.9%
Predominantly cystic	1	11.1%
Signal intensity		
Hyposignal on T1	9	100%
Hypersignal on T2	8	88.9%
Isointense signal on T2	1	11.1%
Hypersignal on FLAIR	7	77.8%
Isointense signal on FLAIR	2	22.2%
Enhancement		
Present	9	100%
Dissemination		
Cerebrospinal fluid	6	66.7%
Luschka's foramen	4	44.4%
Magendie's foramen	1	11.1%
Absent	2	22.2%

n, number of patients; FLAIR, fluid-attenuated inversion recovery.

DISCUSSION

Most frequently medulloblastomas occur in children and adolescents, with a remarkable decrease in the incidence at the second and third decades of life^(8,9). For patients in the age range between zero and 19 years, the mean age where the tumor is diagnosed is 7.9 years, with 57.3% of cases occurring between zero and 10 years of age⁽⁸⁾. The incidence is higher in male individuals, with a male/female ratio = 1.5–2:1⁽⁸⁾. The desmoplastic variant occurs typically in adolescents or young adults^(10,11). In the present study, a female predominance was observed (female/male, 2:1). Such finding may be associated with limitations of the relatively small sample. Differently from the literature^(10,11), 75% of the cases with desmoplastic variant in the

present casuistic occurred in patients with age ≤ 10 years.

The preferential site of this tumor is the posterior fossa midline, the cerebellum being involved in 94.4% of cases, with more than 75% of these cases originating from the cerebellar vermis. A more lateral involvement of the cerebellar hemisphere is typical of cases where this tumor is found in older children, adolescent and young adults. Fifteen to 20% of medulloblastomas in children are found out of the midline. This difference in localization seems to be associated with the migration of undifferentiated cells of the posterior medullary velum into upper and lateral directions^(8,12–14). The desmoplastic variant is preferentially localized in the cerebellar hemisphere^(10,11), however, in the present small series, despite the predominance of the desmoplastic variant, the preferential site of medulloblastoma was the cerebellar vermis. The tumor was found centered in the cerebellar hemisphere in only one case (11.1%), a four-year-old child. It is important to note, however, the median localization of medulloblastomas in the three adolescents included in the present casuistic.

Medulloblastomas are characterized as solid, homogeneous or heterogeneous, contrast-enhancing masses localized in the posterior fossa, either compressing or extending into the IV ventricle. However, several researchers have described atypical findings identified at computed tomography (CT) and MRI^(4,6,15,16). However, differences between the classic and desmoplastic medulloblastomas subtypes associated with signal intensity and pattern of contrast enhancement have not been observed^(16,17). Most of times, according to Meyers et al.⁽¹⁶⁾, medulloblastomas present heterogeneous signal associated with the presence of cysts necrosis, small blood vessels and/or calcifications, presenting from isointense to hypointense signal on T1-weighted, and isointense to hyperintense signal on T2-weighted sequences. The findings of the present study are similar to the above mentioned findings where the tumors present heterogeneous signal in all of the cases, with predominance of hypointense signal on T1- and iso/hyperintense signal on T2-weighted and FLAIR sequences. In the present study, the

Table 3 Medulloblastomas behavior on diffusion sequences and proton spectroscopy.

Case	Diffusion	Proton spectroscopy			
		Naa/Cr ^(STEAM)	Co/Cr ^(STEAM)	ml/Cr ^(STEAM)	Lac ^(PRESS)
1	Restriction	0.72	1.39	0.63	Present
2	Restriction	0.70	2.49	1.92	Present
3	Restriction	< 0.70	4.26	1.19	Absent
4	Restriction	< 0.70	5.87	1.32	Absent
5	Restriction	1.19	2.84	1.26	Absent
6	Restriction	Not performed	Not performed	Not performed	Not performed
7	Restriction	Not performed	Not performed	Not performed	Not performed
8	Restriction	Indeterminate	Indeterminate	Indeterminate	Present
9	Restriction	< 0.70	4.10	0.75	Present

Naa, N-acetyl aspartate; Cr, creatine; Co, choline; ml, myo-inositol; Lac, lactate; STEAM, stimulated echo acquisition mode; PRESS, point resolved spectroscopy.

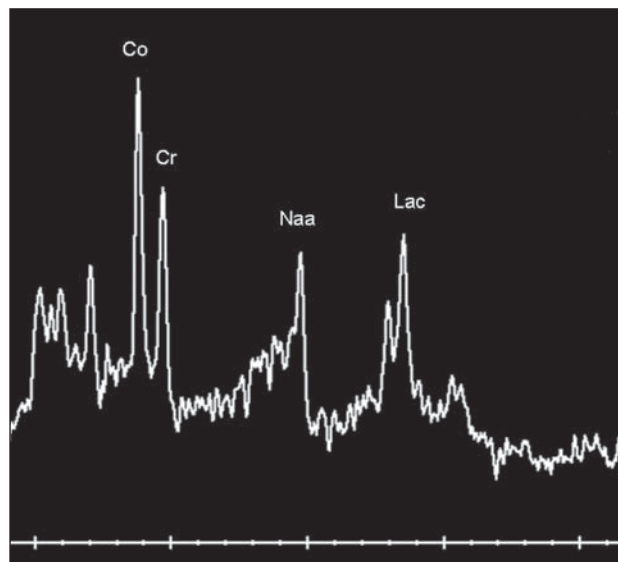


Figure 4. Medulloblastoma in a four-year-old girl. STEAM proton spectroscopy with a single voxel on the tumor lesion demonstrates decrease in the Naa/Cr ratio, increase in the Co/Cr ratio, and presence of Lac peak. The PRESS technique demonstrated Lac peak inversion (not shown).

presence of tumor cysts/necrosis was observed in 100% of cases. Several authors have found the presence of cysts/necrosis in medulloblastomas, with prevalence ranging from 47% to 82% of cases^(4,6,13,18). This difference may be associated with the higher MRI sensitivity for detecting small cysts in the posterior fossa as compared with CT or the variation in the age range found in the different studies. In the present casuistic, only one predominantly cystic tumor was found with peripheral contrast-enhancement. The gadolinium enhancement was heterogeneous and with variable intensity in 100% of cases. In the literature, the level of contrast-enhancement is quite variable, the heterogeneous pattern being considered as a rule⁽¹⁶⁾.

The tumor extension through the IV ventricle drainage foramina has been associated with ependymoma, because of the "plastic" characteristics of this tumor^(2,3). However, medulloblastomas generally grow into and fill the IV ventricle and also may extend through the Magendie's foramen and less frequently through the Luschka's foramina⁽²⁾. According to the literature, 15% of medulloblastomas present tumor extension through the Luschka's and/or Magendie's foramina^(6,17). In the present study, tumor extension through the Luschka's foramen was observed in four cases (44.4%), one of them also involving the Magendie's foramen. These findings emphasize the necessity of including medulloblastoma in the differential diagnosis of tumors affecting the IV ventricle drainage foramina.

The staging of medulloblastomas is based on the tumor size and extent as well as on the presence or not of metastasis through the cerebellar fluid or out of the central nervous system. These tumors present a marked tendency to dissemination through the cerebellar fluid to the whole neuroaxis, affecting the ventricular surfaces, the subarachnoid space and nervous roots^(4,19,20). Dissemination through the cerebellar fluid is identified in about 20%-50% of patients in the initial diagnosis, with diffuse and nodular metastases being frequently found⁽²⁰⁾. Considering the high incidence of dissemination findings at the diagnosis and consequential worsening in the prognosis, imaging evaluation of the

whole neuroaxis is required before the treatment initiation⁽¹⁹⁾. Magnetic resonance images acquired after gadolinium injection have shown to be more sensitive for the diagnosis of subarachnoid dissemination as compared with myelotomography and cerebrospinal fluid cytology^(21,22). According to Meyers et al.⁽²²⁾, leptomeningeal enhancement (representing subarachnoid tumor) was the most specific finding corresponding to tumor dissemination (97%). In the present study, signs of intracranial cerebrospinal fluid dissemination were observed in 66.7% of cases, most of them represented by linear or nodular meningeal enhancement as well as by the presence of intraventricular implant.

Despite the non-specificity of ADC values for evaluating the histology of all types of brain tumors, the application of this parameter in pediatric patients with posterior fossa tumors is indicated⁽²³⁾. The ADC is inversely proportional to the cellular density, presumably secondary to the tortuosity of the interstitial space and to the resulting restriction of water molecules mobility. So, the high lesion cellularity leads to an increase in the diffusion signal and consequently hyposignal on the ADC map^(5,23). In a retrospective analysis of 32 pediatric patients with posterior fossa tumors, Rumboldt et al.⁽²³⁾ have established ADC cut off values where values $> 1.40 \times 10^{-3} \text{ mm}^2/\text{s}$ were 100% specific for juvenile pilocytic astrocytoma, whereas values $< 0.90 \times 10^{-3} \text{ mm}^2/\text{s}$ were 100% specific for medulloblastoma and atypical rabdoid/teratoid tumor; measurements between 1.00 and $1.30 \times 10^{-3} \text{ mm}^2/\text{s}$ were specific for the majority of ependymomas. In a visual, subjective evaluation of the ADC map, these findings correspond to a marked hypersignal for juvenile pilocytic astrocytoma, moderate hypersignal for ependymoma, and hypo- to isosignal for medulloblastoma and atypical rabdoid/teratoid tumor. In 100% of the present casuistic, a visual, subjective evaluation demonstrated areas of restriction to water molecules mobility, i.e., areas of hyposignal on the ADC map, probably associated with the high cellularity of medulloblastomas.

MRI spectroscopy is a non-invasive technique that allows the characterization of the biochemical profile of brain tissues.

Naa is a marker for neuronal density and feasibility that is found at decreased concentrations in tumor lesions supposedly as a result of the replacement of neurons by neoplastic cells. The main Naa peak corresponds to 2.02 ppm. The Co peak reflects the cellular membrane turnover and is increased in the presence of hypercellularity, like in processes involving tumors. This peak corresponds to 3.22 ppm. Myo-inositol (mI) is considered as a marker for glial cells whose peak corresponds to 3.55 ppm. Alteration in this peak is found in the presence of osmolarity disorders, white matter diseases and low-grade neoplasms such as grade II astrocytomas. Creatine levels are relatively constant even under certain pathological conditions, so this marker is utilized as an internal reference. The main Cr peak corresponds to 3.03 ppm. Lac that is typically absent or found at low concentrations, is considered as a product from the anaerobic glucose metabolism, and is found at increased concentrations in tumors because of decreased oxidative respiration. Lac is found at 1.33 ppm, with a double inverted peak on sequences with long echo time (around 135 ms). Therefore, decreased Naa peak, increase in Co and Mi peaks, and detection of the Lac peak are typical findings at proton spectroscopy for primary neoplasms^(5,24). According to Costa⁽⁷⁾, proton spectroscopy has allowed the differentiation among the three main types of tumor affecting the posterior fossa in the pediatric age range. This author has concluded that medulloblastoma demonstrated the higher Co/Cr and Co/Naa ratios as compared with pilocytic astrocytoma and ependymoma. In the present study, the authors have demonstrated a decrease in the Naa/Cr ratio in 83.3% of cases, and increase in Co/Cr and mI/Cr ratios in respectively 100% and 66.7% of cases. Additionally, the Lac peak was demonstrated in 57.1% of the tumors.

Diffusion sequence and proton spectroscopy findings should always be correlated with conventional MRI findings. The set of macroscopic MRI findings added to the biochemical characteristics of medulloblastomas, although non-specific, have been useful in the differentiation of the main types of posterior fossa tumors, improving the diagnostic accuracy. It is important to

note the relevance of these findings for an appropriate staging and therapy planning to improve the prognosis of these patients.

CONCLUSION

Typically, medulloblastomas present like predominantly solid tumors centered on the posterior fossa midline, with heterogeneous signal and predominance of hyposignal on T1-weighted sequences, and iso/hypersignal on T2-weighted sequences. Gadolinium-based contrast enhancement is frequent and heterogeneous, and tumor dissemination through the cerebrospinal fluid is frequently found. However, the authors observed atypical findings associated with these tumors, such as cysts/tumor necrosis and tumor extension to the IV ventricle drainage foramina. The finding of limited diffusion of water molecules suggests the diagnosis of medulloblastoma, while spectroscopy demonstrates a pattern of tumor lesion.

REFERENCES

1. Becker LE. Pathology of pediatric brain tumors. *Neuroimaging Clin N Am.* 1999;9:671–90.
2. Smirniotopoulos JG. The new WHO classification of brain tumors. *Neuroimaging Clin N Am.* 1999; 9:595–613.
3. Luh GY, Bird CR. Imaging of brain tumors in the pediatric population. *Neuroimaging Clin N Am.* 1999;9:691–716.
4. Sandhu A, Kendall B. Computed tomography in management of medulloblastomas. *Neuroradiology.* 1987;29:444–52.
5. Al-Okaili RN, Krejza J, Wang S, et al. Advanced MR imaging techniques in the diagnosis of intraaxial brain tumors in adults. *Radiographics.* 2006;26:173–89.
6. Mueller DP, Moore SA, Sato Y, et al. MRI spectrum of medulloblastoma. *Clin Imaging.* 1992;16: 250–5.
7. Costa MO. Estudo por imagens convencionais e espectroscopia de prótons por ressonância magnética dos tumores da fossa posterior na faixa etária pediátrica [tese de doutorado]. São Paulo: Faculdade de Medicina da Universidade de São Paulo; 2003.
8. Roberts RO, Lynch CF, Jones MP, et al. Medulloblastoma: a population-based study of 532 cases. *J Neuropathol Exp Neurol.* 1991;50:134–44.
9. Reis Filho JS, Gasparetto EL, Faoro LN, et al. Medulloblastomas: achados clínicos, epidemiológicos e anátomo-patológicos de 28 casos. *Arq Neuropsiquiatr.* 2000;58:76–80.
10. Stávale JN, Cruz JRS. Medulloblastoma desmoplásico: fatores histológicos de prognóstico. *Arq Neuropsiquiatr.* 1993;51:487–90.
11. Levy RA, Blaivas M, Muraszko K, et al. Desmoplastic medulloblastoma: MR findings. *Am J Neuroradiol.* 1997;18:1364–6.
12. Koeller KK, Rushing EJ. From the archives of the AFIP: medulloblastoma: a comprehensive review with radiologic-pathologic correlation. *Radiographics.* 2003;23:1613–37.
13. Bourgouin PM, Tampieri D, Grahovac SZ, et al. CT and MR imaging findings in adults with cerebellar medulloblastoma: comparison with findings in children. *AJR Am J Roentgenol.* 1992; 159:609–12.
14. Nelson M, Diebler C, Forbes WS. Paediatric medulloblastoma: atypical CT features at presentation in the SIOP II trial. *Neuroradiology.* 1991; 33:140–2.
15. Barkovich AJ. Intracranial, orbital, and neck tumors of childhood. In: Barkovich AJ, editor. *Pediatric neuroimaging.* Philadelphia: Lippincott Williams & Wilkins; 2000. p. 443–580.
16. Meyers SP, Kemp SS, Tarr RW. MR imaging features of medulloblastomas. *AJR Am J Roentgenol.* 1992;158:859–65.
17. Tortori-Donati P, Fondelli MP, Rossi A, et al. Medulloblastoma in children: CT and MRI findings. *Neuroradiology.* 1996;38:352–9.
18. Carvalho Neto A, Gasparetto EL, Ono SE, et al. Adult cerebellar medulloblastoma: CT and MRI findings in eight cases. *Arq Neuropsiquiatr.* 2003; 61:199–203.
19. Packer RJ, Cogen P, Vezina G, et al. Medulloblastoma: clinical and biologic aspects. *Neuro Oncol.* 1999;1:232–50.
20. Osborn AG. Meningeomas e outras neoplasias não gliais. In: Osborn AG, editor. *Diagnóstico neuroradiológico.* Rio de Janeiro: Revinter; 1999. p. 579–625.
21. Heinz R, Wiener D, Friedman H, et al. Detection of cerebrospinal fluid metastasis: CT myelography or MR? *AJNR Am J Neuroradiol.* 1995;16: 1147–51.
22. Meyers SP, Wildenhain SL, Chang JK, et al. Postoperative evaluation for disseminated medulloblastoma involving the spine: contrast-enhanced MR findings, CSF cytologic analysis, timing of disease occurrence, and patient outcomes. *AJNR Am J Neuroradiol.* 2000;21:1757–65.
23. Rumboldt Z, Camacho DLA, Lake D, et al. Apparent diffusion coefficients for differentiation of cerebellar tumors in children. *AJNR Am J Neuroradiol.* 2006;27:1362–9.
24. Wang ZJ, Zimmerman RA. Proton MR spectroscopy of pediatric brain metabolic disorders. *Neuroimaging Clin N Am.* 1998;8:781–807.